

Research Article

Single-Chain Conformation for Interacting Poly(N-isopropylacrylamide) in Aqueous Solution

Boualem Hammouda¹, Di Jia², and He Cheng²

¹National Institute of Standards and Technology, Center for Neutron Research, 100 Bureau Drive, Gaithersburg, MD 20899-6102, USA

²China Spallation Neutron Source, Institute of High Energy Physics, Chinese Academy of Sciences, Dongguan Institute of Neutron Science, Dongguan, China, 523803

Corresponding Author: Boualem Hammouda; email: hammouda@nist.gov

Received 1 December 2014; Accepted 29 December 2014

Academic Editors: Ruggero Angelico, Bo-Tau Liu, Demeter Tzeli, and Jianling Zhang

Copyright © 2015 Boualem Hammouda et al. This is an open access article distributed under the Creative Commons Attribution License, which permits unrestricted use, distribution, and reproduction in any medium, provided the original work is properly cited.

Abstract. The demixing phase behavior of Poly(N-isopropylacrylamide) (PNIPAM) aqueous solution is investigated using small-angle neutron scattering. This polymer phase separates upon heating and demixes around 32 °C. The pre-transition temperature range is characterized by two scattering modes; a low-Q (large-scale) signal and a high-Q dissolved chains signal. In order to get insight into this pre-transition region, especially the origin of the low-Q (large-scale) structure, the zero average contrast method is used in order to isolate single-chain conformations even in the demixing polymers transition region. This method consists of measuring deuterated and non-deuterated polymers dissolved in mixtures of deuterated and non-deuterated water for which the polymer scattering length density matches the solvent scattering length density. A fixed 4% polymer mass fraction is used in a contrast variation series where the d-water/h-water fraction is varied in order to determine the match point. The zero average contrast (match point) sample displays pure single-chain scattering with no interchain contributions. Our measurements prove that the large scale structure in this polymer solution is due to a transient polymer network formed through hydrophobic segment-segment interactions. Scattering intensity increases when the temperature gets close to the phase boundary. While the apparent radius of gyration increases substantially at the Lower Critical Solution Temperature (LCST) transition due to strong interchain correlation, the single-chain true radius of gyration has been found to decrease slightly with temperature when approaching the transition.

Keywords: PNIPAM, SANS, zero average contrast, LCST, phase transition, water-soluble polymer

1. Introduction

Poly(N-isopropylacrylamide) polymer also referred to as PNIPAM has attracted much research interest. PNIPAM can undergo a coil-to-globule transition with varying temperature [1, 2] and is known for co-nonsolvation when dissolved in water/ethanol mixtures [3]. Co-nonsolvation means that

the polymer demixes in solvent mixtures while it mixes well in the individual solvents. The co-nonsolvation work used small-angle neutron scattering (SANS) to map out the demixing phase diagram. PNIPAM passes through a re-entrant behavior with the addition of a co-nonsolvent [4, 5]. Both effects of solvent quality (from good to theta solvent)

and concentration effect can be seen in semi-dilute PNIPAM aqueous solution when varying temperature.

SANS measurements have been used to investigate the non-mean field behavior of the lower critical solution transition (LCST) in semidilute PNIPAM solution in deuterated water (d-water) [6]. Critical exponents were measured. Time-dependent kinetics measurements were made following a temperature jump from the mixed phase into the (higher temperature) demixed phase regions. The LCST transition is driven by the squeezing out of water molecules from the hydration region around the polymer.

Since this is not a review paper, we did not feel necessary to thoroughly review the published literature regarding PNIPAM. We preferred instead to keep this paper focused on single-chain conformations using SANS and the zero average contrast method. We did not find many investigations of PNIPAM solutions using SANS.

2. Demixing Polymer Morphology

In our previous investigation of the co-nonsolvation of PNIPAM in d-water/d-ethanol mixtures, we had noticed an interesting pre-demixing behavior for 4% mass fraction PNIPAM solution in d-water [3]. This trend is reproduced in Figure 1. The LCST is between 30 °C and 35 °C. Temperatures below 30 °C correspond to typical buildup of composition fluctuations when approaching a phase transition in polymer solutions. The 35 °C temperature corresponds clearly to a demixed solution while the case for 30 °C shows an interesting pre-transition behavior characterized by the high-Q ($\sim 1/Q^2$) feature representing dissolved chains in addition to a form of low-Q aggregation feature ($\sim 1/Q^{2.03}$).

In order to investigate the polymer chain conformations before, during, and after the demixing transition, we decided to apply the so-called zero average contrast method in conjunction with small-angle neutron scattering (SANS). This method consists in measuring a mixture of deuterated and non-deuterated (hydrogenated) polymers in a mixture of deuterated and hydrogenated water where the average solvent scattering length density matches the average scattering length density of the polymers. This matching condition corresponds to the zero average contrast. At this condition, scattering is proportional to the polymer single-chain form factor.

3. The Zero Average Contrast Method

The SANS cross section for a mixture of deuterated and hydrogenated polymers in water is given by:

$$\frac{d\Sigma(Q)}{d\Omega} = (\rho_{dP} - \rho_S)^2 S_{DD}(Q) + (\rho_{hP} - \rho_S)^2 S_{HH}(Q) + 2(\rho_{dP} - \rho_S)(\rho_{hP} - \rho_S) S_{HD}(Q). \quad (1)$$

ρ_{dP} , ρ_{hP} , and ρ_S are the scattering length densities for the deuterated polymer, hydrogenated polymer and solvent respectively, $S_{DD}(Q)$, and $S_{HH}(Q)$ are the scattering factors for a pair of deuterated polymers and a pair of hydrogenated polymers respectively and $S_{HD}(Q)$ is the cross term.

Assuming that deuterated and hydrogenated polymers have the same degree of polymerization ($n_{dP} = n_{hP} = n_P$), and the same monomer volume ($v_{dP} = v_{hP} = v_P$), and defining the polymer volume fraction as $\phi_P = \phi_{dP} + \phi_{hP}$, one can split single-chain and interchain contributions and recombine the cross section into the following form [7, 8].

$$\frac{d\Sigma(Q)}{d\Omega} = (\rho_{dP} - \rho_{hP})^2 \frac{\phi_{dP}\phi_{hP}}{\phi_P^2} n_P \phi_P v_P P_S(Q) + (\rho_P - \rho_S)^2 n_P \phi_P v_P P_T(Q). \quad (2)$$

The scattering length density for the deuterated/hydrogenated polymer mixture is $\rho_P = \rho_{dP}\phi_{dP}/\phi_P + \rho_{hP}\phi_{hP}/\phi_P$ while that for the deuterated/hydrogenated solvent mixture is $\rho_S = \rho_{dS}\phi_{dS}/\phi_S + \rho_{hS}\phi_{hS}/\phi_S$. Setting the second contrast factor (between the polymer and the solvent) to zero cancels out the second term containing the interchain contributions $P_T(Q)$ leaving only the first term containing the single-chain form factor $P_S(Q)$. Using a series of deuterated/hydrogenated solvent mixtures, one reaches a minimum in the cross section at the zero average contrast condition. That minimum corresponds to $\rho_P = \rho_S$. In our case, dPNIPAM/hPNIPAM isotopic polymer mixtures are dissolved in d-water/h-water solvent mixtures. The zero average contrast method works only for homogeneously mixed samples.

The synthesis and NMR and GPC characterizations of deuterated and hydrogenated PNIPAM polymers are described next.

4. Synthesis of Deuterated NIPAM Monomer

Relevant synthesis details are described briefly here. A quantity of 3.94 g of sodium hydroxide was mixed in 6.6 mL of pure water. Some 13 mL of dichloromethane and 6.6 mL of isopropyl-1,1,1,3,3,3- d_6 -amine were added and the flask was placed in an ice water bath. Then 5.64 mL of acryloylchloride dissolved in 3.76 mL of dichloromethane were added dropwise with slow stirring. The reaction was allowed to run for 6 h in an ice water bath and for another 12 h at room temperature. When the reaction was finished, a funnel was used to separate out the organic phase from the water phase; the organic phase was then washed using saturated sodium chloride aqueous solution several times and then dried using anhydrous magnesium. Finally, rotary evaporation was used to remove dichloromethane. 2D nuclear magnetic resonance (NMR) was used to prove that the deuterated NIPAM was synthesized successfully.

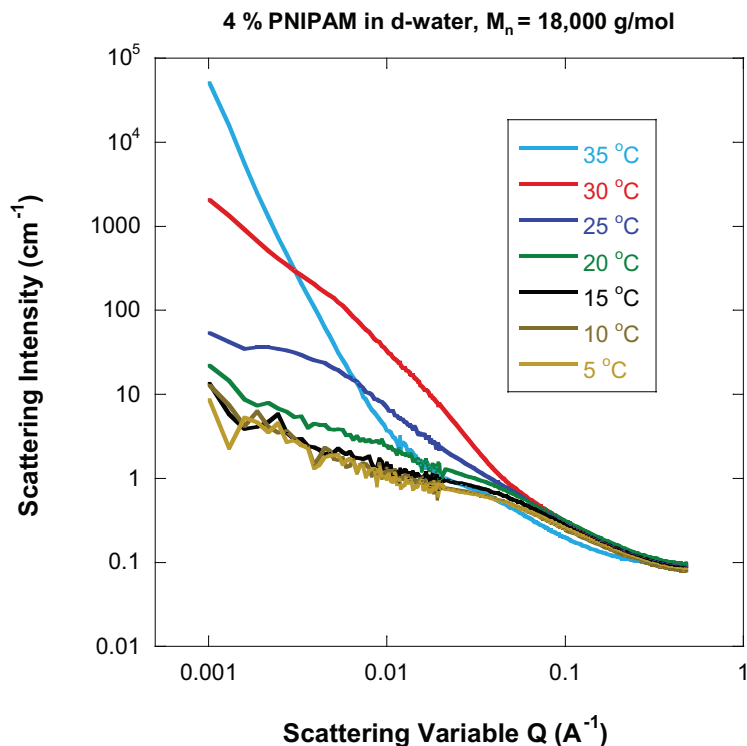


Figure 1: The scattering intensity for 4% mass fraction PNIPAM ($M_n = 18,000$ g/mol) in d-water increases for increasing temperature, showing LCST behavior. The sample is clearly dissolved for temperatures below 30 °C and clearly demixed for 35 °C.

5. Synthesis of Deuterated PNIPAM Polymers

The deuterated PNIPAM chain was synthesized by reversible addition-fragmentation chain-transfer (RAFT) reaction. The molar ratios of the reactants for deuterated NIPAM: CDB(cumyl dithiobenzoate) (chain transfer agent): AIBN (initiator) were 500:1:0.2. Quantities of 3.0000 g deuterated NIPAM, 0.0144 g CDB and 0.0017 g AIBN were dissolved in 3 mL DMF, the mixture was added in a polymerization tube. The tube was first frozen and thawed three times to remove oxygen, then put in an oil bath at 60 °C with a stirring speed of 6.7 Hz (6.7 revolutions per second or 400 rpm) for 24 hrs. After reacting, the product was precipitated in a large amount of ether to get rid of unreacted monomer and initiator. Finally, the product was dried in a vacuum oven at room temperature overnight.

The synthesis of hydrogenated PNIPAM polymers was the same as that for deuterated PNIPAM except for the use of non-deuterated monomer.

6. NMR Characterization

2D Nuclear Magnetic Resonance (NMR) was used to confirm that deuterated NIPAM had been successfully synthesized, as shown in Figure 2.

7. GPC Characterization

Gel Permeation Chromatography (GPC) was conducted to characterize the molecular weight of the deuterated, hydrogenated and mixture of deuterated and hydrogenated PNIPAM polymers. Table 1 shows that both deuterated and hydrogenated PNIPAM are mono-dispersed.

8. Samples Prepared for SANS

All the prepared samples contained 4% mass fraction PNIPAM polymer and are marked in Figure 3. Sample 13 contains 4% hPNIPAM mass fraction in d-water, while sample 15 contains 4% dPNIPAM mass fraction in h-water. These correspond to maximum sample contrasts. A series of 12 samples containing 50% dPNIPAM/50% hPNIPAM fractions with varying d-water/h-water fractions were prepared. These correspond to 100% d-water (and 0% h-water) for sample 1, 10% d-water for sample 2, 20% d-water for sample 3, etc, till 0% d-water (and 100% h-water) for sample 12. An extra sample with 67.5% d-water (sample 5) was also prepared. One of the samples in this series will correspond to the zero average contrast condition.

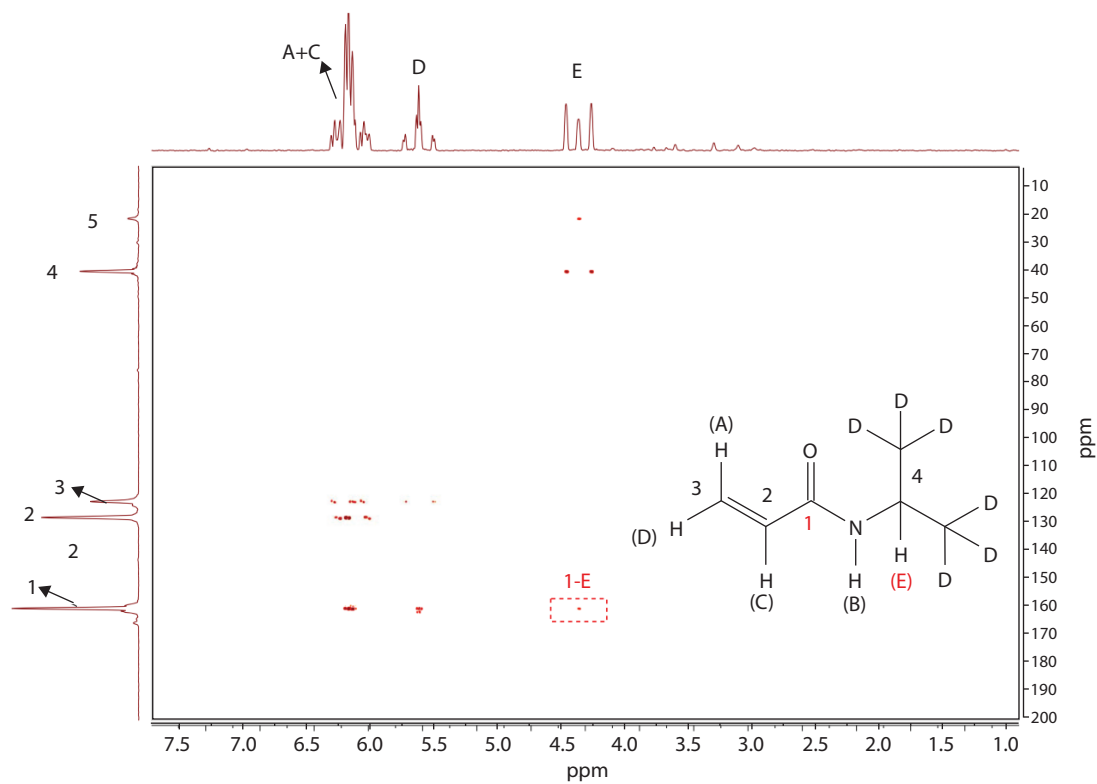
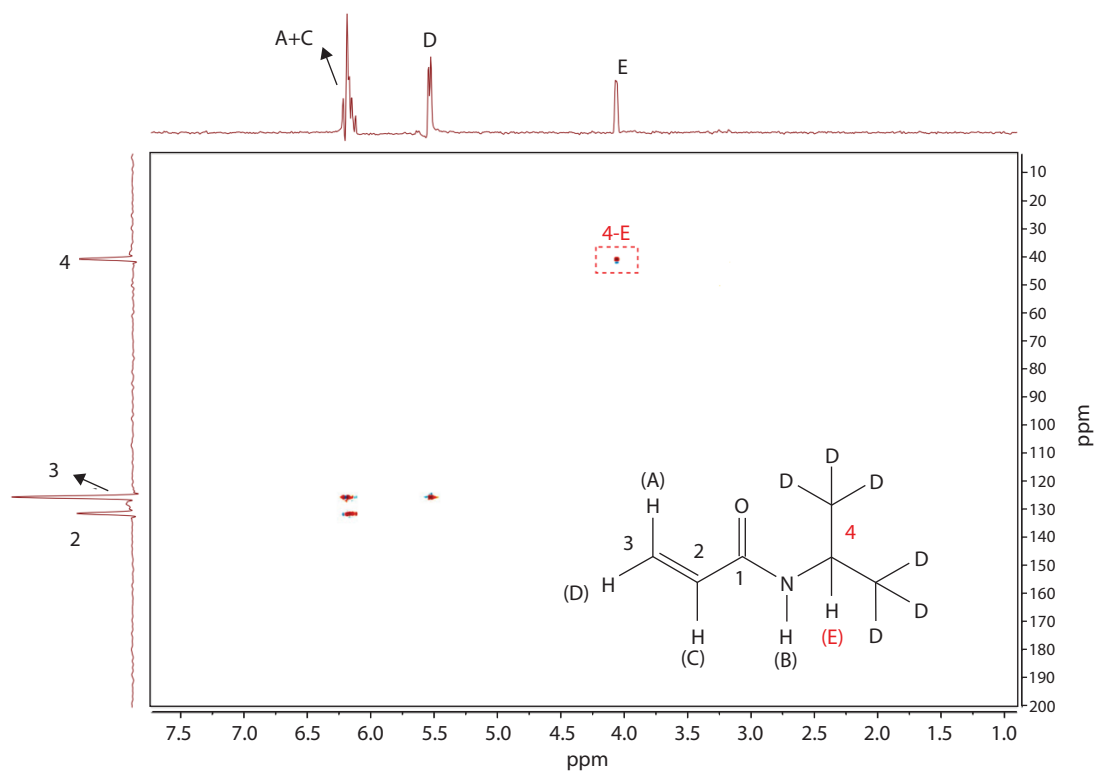


Figure 2: 2D NMR of deuterated NIPAM: (a) one bond ^1H - ^{13}C correlated spectroscopy, and (b) three bond ^1H - ^{13}C correlated spectroscopy.

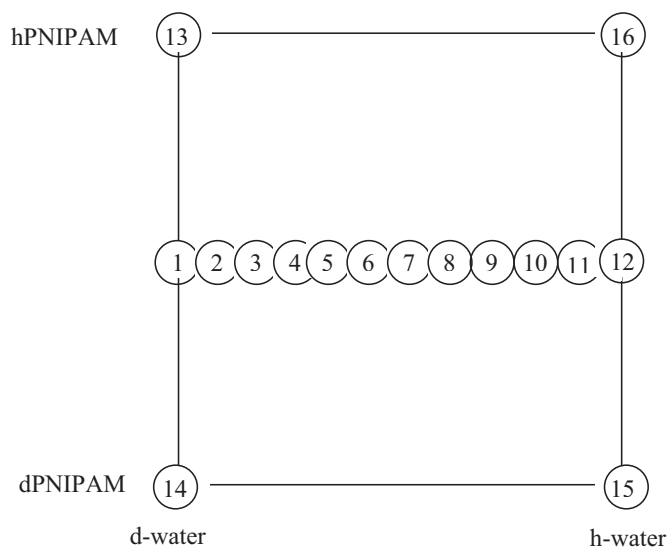


Figure 3: List of samples prepared. Samples 13 and 14 contain d-water as solvent while samples 16 and 15 contain h-water as solvent.

Table 1: GPC characterization of deuterated, hydrogenated and mixture of both PNIPAM polymers (THF was used as eluent and PS was used as standard). M_n and M_w are the number average and mass average molecular masses and M_p is the molecular mass of the highest peak.

Sample Name	M_n	M_w	M_p	Polydispersity Index
Hydrogenated PNIPAM	88000	104000	114000	1.18
Deuterated PNIPAM	96000	105000	106000	1.10
Mixture of deuterated and hydrogenated PNIPAM	92000	104000	109000	1.14

9. SANS Data Acquisition and Data Reduction

SANS measurements were performed on the 30 m NG7 instrument at the National Institute of Standards and Technology, Center for Neutron Research. Measurements were taken for three sample-to-detector distances of 1 m, 4 m, and 15.3 m. The neutron wavelengths were 6 Å for the 1 m and 4 m sample-to-detector distances and 8.09 Å for the 15.3 m detector distance. The first two configurations yield a minimum scattering variable $Q_{min} = 0.01 \text{ \AA}^{-1}$ while the last configuration used neutron focusing lenses in order to achieve a lower value of $Q_{min} = 0.001 \text{ \AA}^{-1}$. Standard data acquisition and data reduction methods were used to obtain radially averaged SANS data.

In order to assess whether the zero average contrast method is working, let's plot the scale factor defined as $\text{Scale Factor} = I(Q_{min} = 0.01 \text{ \AA}^{-1}) - I(Q_{max} = 0.5 \text{ \AA}^{-1})$ where the SANS intensity is taken at low-Q (coherent part) and high-Q (incoherent part) for the entire contrast variation series; i.e., for samples 1 to 12. One can see that the trend presents a minimum around sample 8 which corresponds to 40% d-water and that the location of this minimum varies a little bit when temperature is varied from 5 °C, to 15 °C then 25 °C. Sample 8 is therefore the closest to the zero average contrast condition. Statistical error bars correspond to one standard deviation throughout.

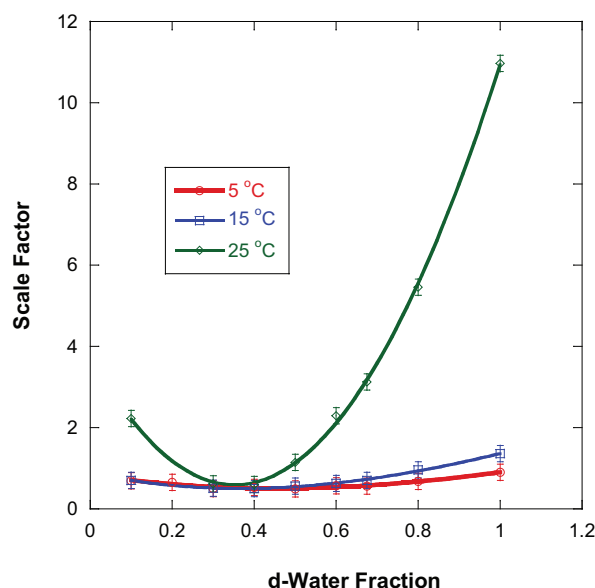


Figure 4: Plot of the SANS Scale Factor for the contrast variation series samples 1 to 12.

At the zero average condition, the second term in (2) cancels out leaving only the first term [8]. In order to verify this condition graphically, let's subtract the minimum value

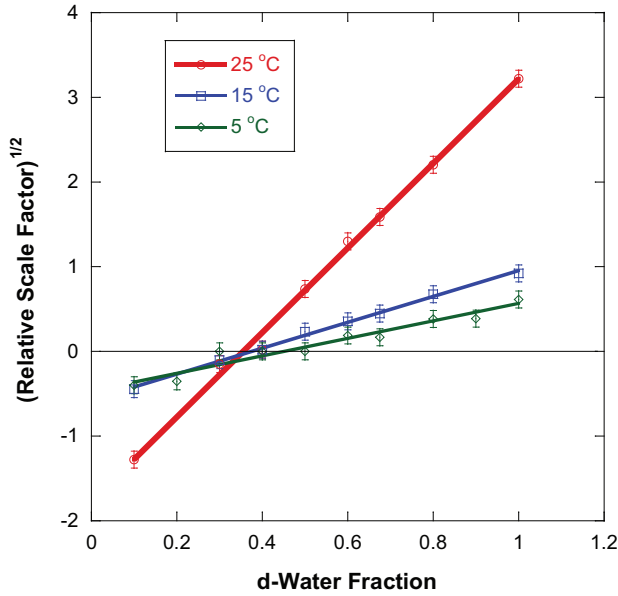


Figure 5: Graphical method to determine the zero average contrast point. The y-axis corresponds to the square root of the relative scale factor (relative to sample 8), equal to $\sqrt{(\text{Scale} - \text{sample 8})}$.

(around sample 8) from the Scale Factor for each of the three temperatures and plot the square root of the difference since the contrast factor involves the square of the scattering length density difference. Instead of a parabolic behavior, the variation becomes linear. Affixing a negative sign in front of the points on the left side of sample 8 yields an uninterrupted line shown in Figure 5. The three lines corresponding to the three temperatures cross the origin of the horizontal axis close to sample 8 thereby confirming the minimum graphically. The fact that data fall on a line (in Figure 5) is a strong indication that the zero average contrast method is working

In order to emphasize the relevance of the zero average contrast condition, let's compare the scattering intensity for sample 13 (hPNIPAM/d-water) and sample 8 (50% dPNIPAM/50% hPNIPAM in 40% d-water/60% hwater) for the measured temperatures in Figure 6. Sample 13 shows large variations due to composition fluctuations (interchain effects) while sample 8 shows very little variation (dashed lines) and characterizes single-chain effects. It clearly demonstrates that the large scale low-Q structure is due to a transient polymer network [9, 10]. Note that the zero average contrast method breaks down for the 35 °C temperature where the sample is phase separated.

For the sake of completeness, the full-Q range SANS data is included for sample 13 with increasing temperature in Figure 7. The low-Q signal is very noisy for weak scattering conditions such as at low temperature. One can notice that Fig 1 and Fig 7 corresponding to different PNIPAM molecular weights are similar.

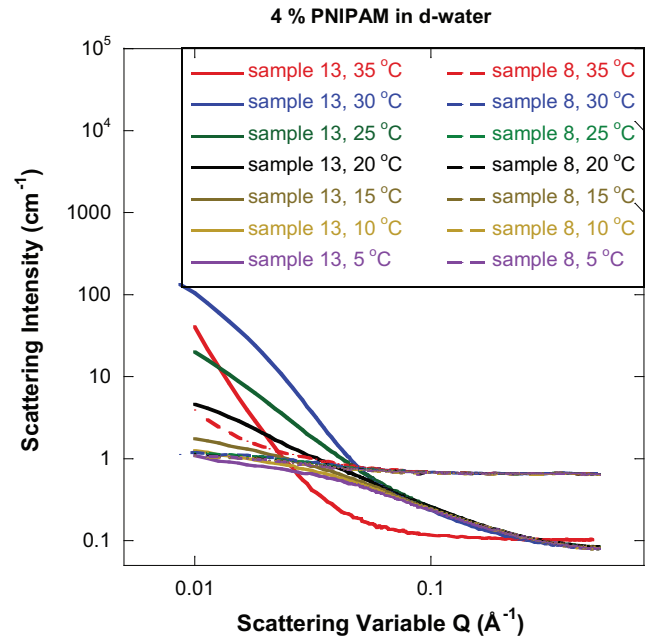


Figure 6: SANS data for sample 13 and for sample 8 at the six measured temperatures. SANS intensity is enhanced when temperature is increased for sample 13 (separated solid lines) while it remains practically constant for sample 8 (overlapping dashed lines) which corresponds to the zero average contrast condition.

In order to analyze the single-chain polymer conformations for sample 1 to sample 12 contrast variation series samples, the Gaussian chain polymer model with excluded volume is used.

10. Single-Chain Conformations with Excluded Volume

The form factor for polymer chains with excluded volume is given by [11, 12].

$$P(Q) = \frac{1}{\sqrt{U}^{1/2\nu}} \gamma\left(\frac{1}{2\nu}, U\right) - \frac{1}{\sqrt{U}^{1/\nu}} \gamma\left(\frac{1}{\nu}, U\right). \quad (3)$$

Here, $\gamma(x, U)$ is the incomplete gamma function:

$$\gamma(x, U) = \int_0^U dt \exp(-t)t^{x-1}. \quad (4)$$

The variable U is given in terms of the scattering variable Q as:

$$U = \frac{Q^2 a^2 n^{2\nu}}{6} = \frac{Q^2 R_g^2 (2\nu + 1)(2\nu + 2)}{6}. \quad (5)$$

Here ν is the excluded volume parameter, a is the polymer chain statistical segment length, n is the degree of polymerization. The radius of gyration squared has been defined as:

$$R_g^2 = \frac{a^2 n^{2\nu}}{(2\nu + 1)(2\nu + 2)} \quad (6)$$

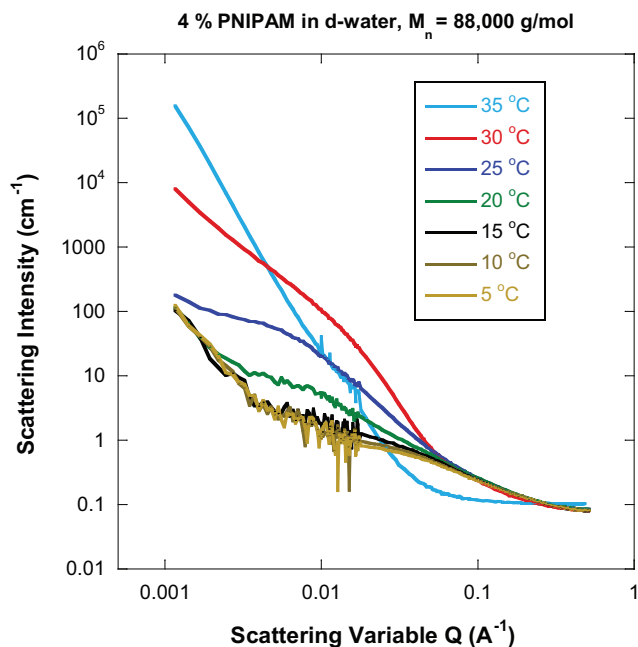


Figure 7: Full SANS data window (with $Q_{min} = 0.001 \text{ \AA}^{-1}$) for sample 13 at the measured temperatures.

This model is used next to analyze SANS data for the contrast variation sample series. The scattering intensity is proportional to this form factor

$$I(Q) = \text{Scale} * P(Q) + B, \quad (7)$$

where B is the (Q -independent) incoherent background. This model describing polymer solutions with excluded volume has become a standard routine in the NIST SANS data analysis package [13].

11. SANS Data Analysis

Figure 7 clearly shows that sample 13 is dominated by the second term in (2) which has contributions from inter-chain scattering while sample 8 is dominated by the first term (single-chain scattering). The Gaussian chain model (with excluded volume) is used to fit SANS data in order to obtain a scale, an apparent radius of gyration and an excluded volume parameter. Fit results of the scale factor (7) shown in Figure 8 show again that sample 13 is dominated by the so-called chi effects while sample 8 is purely single-chain scattering.

Fitting to the Gaussian chain model for sample 13 yields an apparent radius of gyration while for sample 8, it yields the true single-chain radius of gyration. Figure 9 shows that the single-chain radius of gyration decreases with temperature for sample 8 while the apparent radius of gyration increases with temperature for sample 13 due to strong composition fluctuations (chi effects) leading to LCST phase separation. The decrease of some 17% for sample 8 denotes a real single-chain contraction. Note that the Porod exponent (inverse of

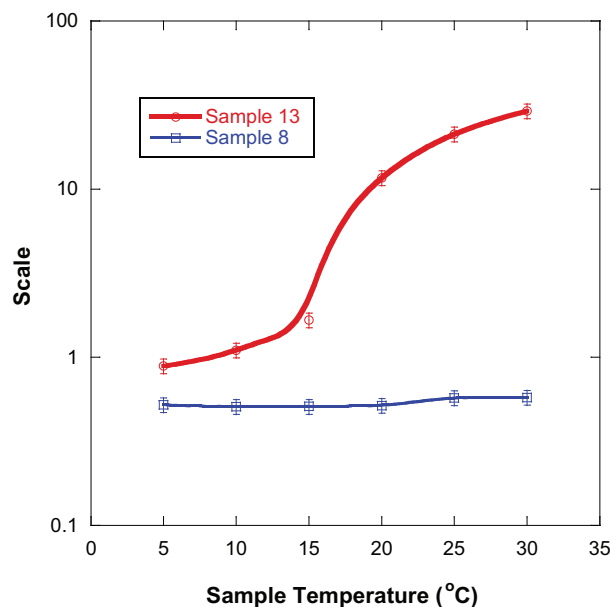


Figure 8: Variation of the intensity Scale parameter obtained from fits to the Gaussian chain with excluded volume for sample 13 and sample 8. Smooth fit lines have been added to guide the eye.

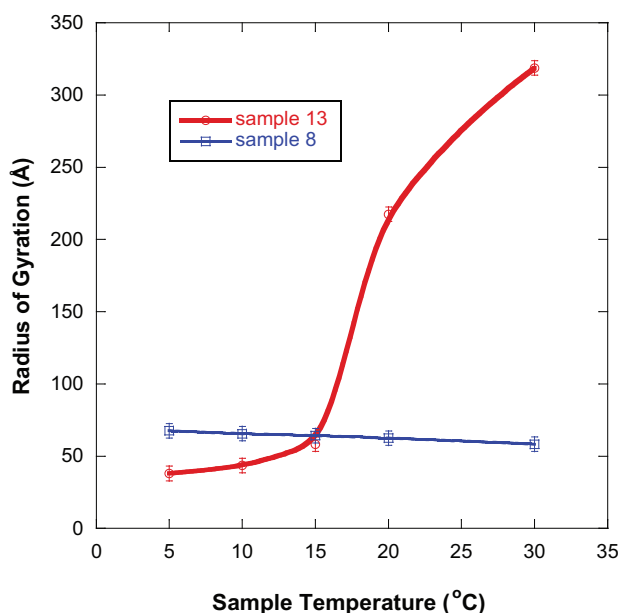


Figure 9: Variation of the apparent radius of gyration for sample 13 and of the single-chain radius of gyration for sample 8.

the excluded volume parameter) is around 2 for sample 8 and increases slightly as the phase transition temperature is approached as it should. It becomes 2.2 at 30 °C.

Figure 10 shows the variation of the apparent radius of gyration for the contrast variation series samples at two temperatures. At the contrast match condition, the radius of gyration is independent of temperature, while for the other conditions (with no contrast match), this is not the case.

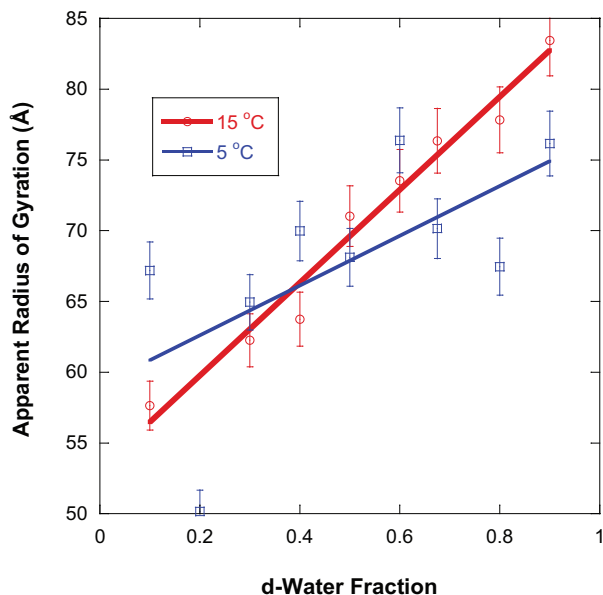


Figure 10: Variation of the apparent radius of gyration for the contrast variation series.

12. Summary and Discussion

PNIPAM phase separates upon heating at around 32 °C. At temperatures below 25 °C, PNIPAM chains are well dissolved. Strong composition fluctuations build up at 25 °C. The transition region between 25 °C and 32 °C is interesting as evidenced by SANS data (see Figure 1 and Figure 7). The SANS intensity increases when fluctuations buildup making this technique a useful probe to investigate the thermodynamics of demixing. In order to understand the nature of this transition region, the zero average contrast method was used on mixtures of dPNIPAM/hPNIPAM and d-water/h-water in order to back out single-chain conformations. This method worked nicely and yielded new results. We found that single-chain conformations change only slightly through the transition region in which composition fluctuations built up substantially. The single-chain radius of gyration actually shrinks slightly while the apparent radius of gyration increases substantially accounting for growing interchain correlations at the onset of phase separation due to chi effects. While approaching the LCST transition from lower temperatures, the demixing transition proceeds in two steps. The pre-transition step involves PNIPAM chain shrinking while the transition itself involves complete demixing driven by chi effects.

Note that another experiment used SANS with the zero average contrast method to investigate single-chain polymer conformation of polystyrene in cyclohexane [14] at the critical composition. They found very small chain contraction as evidenced by a very slight decrease in the single-chain radius of gyration.

Disclaimer/Acknowledgements

The identification of commercial products does not imply endorsement by the National Institute of Standards and Technology nor does it imply that these are the best for the purpose. This work is based upon activities supported in part by the National Science Foundation under Agreement No. DMR-0944772. HC was supported by the Capital (Beijing) Science & Technology Resources Platform (Z131110000613065). Helpful discussions with Charles Han are appreciated.

References

- [1] G. Z. Zhang and C. Wu, Folding and Formation of Mesoglobules in Dilute Copolymer Solutions, *Advances in Polymer Science*, **195**, 101–176, (2006).
- [2] H. Cheng, L. Shen, and C. Wu, LLS and FTIR Studies on the Hysteresis in Association and Dissociation of Poly(N-isopropylacrylamide) Chains in Water, *Macromolecules*, **39**, 2325–2329, (2006).
- [3] M. Hore, B. Hammouda, Y. Li, and H. Cheng, Co-Nonsolvency of Poly(N-isopropylacrylamide) in Deuterated Water/Ethanol Mixtures, *Macromolecules*, **46**, 7894–7901, (2013).
- [4] G. Liu and G. Zhang, Reentrant behavior of poly(N-isopropylacrylamide) brushes in water - Methanol mixtures investigated with a quartz crystal microbalance, *Langmuir*, **21**, no. 5, 2086–2090, (2005).
- [5] J. K. Hao, H. Cheng, P. Butler, L. Zhang, and C. C. Han, *The Journal of Chemical Physics*, **132**, no. 15, Article ID 154902, (2010).
- [6] A. Meier-Koll, V. Pipich, P. Busch, C. M. Papadakis, and P. Müller-Buschbaum, Phase separation in semidilute aqueous poly(N-isopropylacrylamide) solutions, *Langmuir*, **28**, no. 23, 8791–8798, (2012).
- [7] B. Hammouda, D. Ho, and S. Kline, SANS from poly(ethylene oxide)/water systems, *Macromolecules*, **35**, no. 22, 8578–8585, (2002).
- [8] B. Hammouda, SANS from homogeneous polymer mixtures: A unified overview, *Advances in Polymer Science*, **106**, 86–133, (1993).
- [9] G. Yuan, X. Wang, C. C. Han, and C. Wu, Reexamination of slow dynamics in semidilute solutions: From correlated concentration fluctuation to collective diffusion, *Macromolecules*, **39**, no. 10, 3642–3647, (2006).
- [10] J. Li, T. Ngai, and C. Wu, The slow relaxation mode: From solutions to gel networks, *Polymer Journal*, **42**, no. 8, 609–625, (2010).
- [11] H. Benoit, *Comptes Rendus*, **245**, 2244–2247, (1957).
- [12] B. Hammouda, SANS from homogeneous polymer mixtures: A unified overview, *Advances in Polymer Science*, **106**, 86–133, (1993).
- [13] S. R. Kline, Reduction and analysis of SANS and USANS data using IGOR Pro, *Journal of Applied Crystallography*, **39**, no. 6, 895–900, (2006).
- [14] Y. B. Melnichenko and G. D. Wignall, Dimensions of polymer chains in critical semidilute solutions, *Physical Review Letters*, **78**, no. 4, 686–688, (1997).

Editor-in-Chief
Mostafa Z. Badr, USA

Geographical Editors
Christopher Corton, USA
Jörg Mey, Spain
Marcelo H. Napimoga, Brazil
Nanping Wang, China

Associate Editors

Leggy A. Arnold, USA
Yaacov Barak, USA
Thomas Burris, USA
Ignacio Camacho-Arroyo, Mexico
John Cidlowski, USA
Lluís Fajas Coll, Switzerland
Frédéric Flamant, France
Mario Galigniana, Argentina
Jan-Åke Gustafsson, USA
Anton Jetten, USA
Stafford Lightman, UK
Jian-xing Ma, USA
Sridhar Mani, USA
Iain J. McEwan, UK
Antonio Moschetta, Italy
Bryce M. Paschal, USA
Didier Picard, Switzerland
Ralph Rühl, Hungary
Bart Staels, France
Jiemin Wong, China
Wen Xie, USA

Editorial Board

Brian J. Aleskievich, USA
Jeffrey Arterburn, USA
Frank Beier, Canada
Robert G. Bennett, USA
Carlos Bocos, Spain
Julius Brtko, Slovakia
Moray Campbell, USA
Thomas Chang, Canada
Taosheng Chen, USA
Hueng-Sik Choi, Republic of Korea
Colin Clyne, Australia
Austin Cooney, USA
Pietro Cozzini, Italy
Maurizio Crestani, Italy
Paul D. Drew, USA
Nouridine Faresse, Switzerland
Grace Guo, USA
Heather Hostetler, USA
Wendong Huang, USA
Young Jeong, USA
Hiroki Kakuta, Japan
Yuichiro Kanno, Japan
Jae B. Kim, Republic of Korea
Douglas Kojetin, USA
Christopher Lau, USA
Antigone Lazou, Greece
Chih-Hao Lee, USA
Xiaoying Li, China
Yong Li, China
Nick Z. Lu, USA
Makoto Makishima, Japan
Goldis Malek, USA
Shaker A. Mousa, USA
Zafar Nawaz, USA
Noa Noy, USA
Sergio A. Onate, Chile
Eric Ortlund, USA
Richard P. Phipps, USA
Eric Prossnitz, USA
Brian G. Rowan, USA
Enrique Saez, USA
Edwin R. Sanchez, USA
Andrea Sinz, Germany
Knut Steffensen, Sweden
Cecilia Williams, USA
Bingfang Yan, USA
Xiao-kun Zhang, USA
Chun-Li Zhang, USA
Changcheng Zhou, USA

Nuclear Receptor Research

About the Journal

Nuclear Receptor Research is a peer-reviewed open access journal that publishes high-quality, original research and review articles covering all aspects of research involving all members of the nuclear receptor superfamily.

The editorial board of *Nuclear Receptor Research* has over 70 scientists representing a wide-scope of interest and expertise in the field, from 20 countries around the world.

Nuclear Receptor Research has a fully automated Manuscript Management System (MMS) which makes submission and reviewing as well as tracking of manuscripts an easy, efficient and prompt process to the advantage of the authors. Published articles in *Nuclear Receptor Research* are available in different formats including full-text HTML, full-text PDF, full-text ePUB, full-text XML, and Mobi.

Free Advertising

100% Free of Charge

Advertise, in *Nuclear Receptor Research*, positions available in your laboratory, a position you are seeking, supplies and equipment as well as meetings and conferences related to the field of nuclear receptor research.

For more information about advertising in *Nuclear Receptor Research* please visit the journal website at: <http://www.agialpress.com/journals/nrr/>

For advertising in *Nuclear Receptor Research* please send your ad to nrr.ad@agialpress.com

Contact

Editor-in-Chief: badrm@umkc.edu

Editorial Office: nrr@agialpress.com



100% Free of Charge